Hindawi
Geofluids
Volume 2022, Article ID 9944867, 10 pages
https://doi.org/10.1155/2022/9944867

Research Article

Nanoconfined Bulk-Gas Transport Behavior over a Wide Range of Knudsen Number

Yi Zhang

College of Biology and Agriculture (College of Food Science and Technology), Zunyi Normal University, 563006, China

Correspondence should be addressed to Yi Zhang; sciyiyi@126.com

Received 9 March 2022; Revised 30 March 2022; Accepted 6 April 2022; Published 27 April 2022

Academic Editor: Zheng Sun

Shale matrix, located at Guizhou Province, is rich in nanopores, and gas slippage takes place during shale gas development, resulting in inapplicability of the classical Navier-Stokes equation. Investigation of gas transmission mechanism in nanoscale is helpful to reach a clear understanding of shale gas production performance. On the basis of the Knudsen number, the gas flow mechanism is divided into continuous flow, slippage flow, transition flow, and Knudsen diffusion. Notably, the accurate characterization of transition flow is still challenging up to date. Although there are many established models, they either fail to cover all the flow mechanisms or contain many fitting parameters, the determination of which requires a large number of experimental and molecular simulation data, limiting application of the existing models. Therefore, establishment of bulk-gas transport model over a wide range of Knudsen number without fitting parameters is urgent. First of all, existed theoretical models are compared, and the advantages and disadvantages of previous contributions are analyzed. Weight factors of Knudsen diffusion and slippage flow are obtained, respectively, according to Knudsen's model and Wu's model. Then, a model, free of empirical coefficients, is proposed. After that, effects of pore size, reservoir pressure, and temperature on transmission capacity are investigated. As the proposed model does not contain fitting parameters and remains high accuracy over a wide range of Knudsen number, it shares broad application potential, like shale gas production prediction, reserve estimation in Guizhou Province.

1. Introduction

With decline of global reserves of conventional oil and gas resources, as one of the potential alternative energy resources, shale gas development is the frontier and hotspot [1, 2]. In Guizhou Province, shale gas development will be great help to reduce coal emission and enhance local economic level. However, the corresponding development technology, equipment, and theory are still weak, especially the understanding of pore diffusion mechanism in shale matrix, which makes it difficult to predict shale gas production performance [3]. In view of great difference of gas transport mechanism at different pore scales, it is necessary to elaborate the pore size range in shale gas reservoirs. Fu et al. believe that the pore size in coal matrix is less than 100 nm [4]. Meanwhile, Özgen Karacan [5] and Siriwardane et al. [6] indicated that pore diameter of coal matrix is less than 10 nm. The shale porosity is fairly small, and the permeability falls into the nano-Darcy level. Howard [7] reported that the pore radius in shale ranges from 5 to 15 nm. Katsube [8] found that pore radius of shale, with buried depth of 4400~4500 m, is mainly between 2.7 and 11.5 nm. Reed et al. [9] and Wang and Reed [10] believed that pore radius of shale matrix is between 5 and 1000 nm, and Nelson [11] measured that the minimum pore radius of shale is about 5 nm. As a result, the abundant existence of nanopores in shale is demonstrated.

At nanoscale, fluid slippage takes place, resulting in the inapplicability of classical Navier-Stokes equation [12]. According to the range of Knudsen number, gas flow mechanism is generally divided into continuous flow, slippage flow, transition flow, and Knudsen diffusion. In detail, intermolecular collision dominates continuous flow, while molecule-wall collision dominates the Knudsen diffusion. Because both flow mechanisms are relatively simple, mature theories have been formed at home and abroad [13–15].

With the decrease of pressure or the shrinkage of flow channel, the collision frequency between gas molecules and wall increases gradually, and the gas flow mechanism changes from the continuous flow to slippage flow [15]. Aiming at the characterization method of gas nanopore slippage flow mechanism, Maxwell [16] proposed the first-order boundary condition to modify the Navier-Stokes equation. When $Kn < 0.1$, the proposed equation fits well with the experimental results. Utilizing the first-order boundary condition, Kennard [17], Ebert and Sparrow [18], and Spiga [19] analyzed the characteristics of gas slippage flow in nanopores with different pore geometry. When $Kn > 0.1$, there is a great difference between the experimental observations and the first-order condition, indicating that the first-order boundary conditions are not enough to describe the gas slippage effect [20, 21]. Many scholars successively put forward second-order boundary conditions, hoping that the modified equation can be applied to higher Kn. However, considering the second-order boundary conditions will make the form of the modified equation complex. Finally, the analytical solution can accurately characterize its flow characteristics, and its application range perfectly covers the whole slippage flow [22–27]. The accurate description of transition flow is not only a difficulty at home and abroad but also a key problem to be solved in establishing a bulk-gas transport model covering entire Kn range. Molecular simulation is generally used to study the mechanism of transition flow [28–31]. However, despite the rapid development of computer technology, molecular simulation is still limited by time-consuming calculation, and it cannot be applied to the field.

Adzumi studied the flow characteristics of gas in capillary through a large number of experiments and proposed that the determination of fluid flow mechanism depends on Knudsen number. With the use of weight factor, Adzumi coupled viscous flow and Knudsen diffusion to characterize gas flow behavior in the entire Kn range for the first time. Unfortunately, Adzumi failed to elaborate the expression of the weight factor [32–34]. Liu [35] gave the specific expression of the weight factor on this basis, but the established bulk phase transmission model is only limited to the case when the Kn is less than 1. Liu et al. [36] utilized the weight factor to couple Knudsen diffusion and Fick diffusion, but the weight factor proposed by Liu et al. will not change with Kn. Javadpour [37–39] combined slippage flow and Knudsen diffusion linearly, but it contains an empirical coefficient. Based on the basic theory proposed by Adzumi, Aguilera et al. [40] gave the corresponding weight coefficient expression, but it contains three empirical coefficients. Beskok [32] corrected the slippage flow by introducing the gas rarefaction coefficient and extended the formula to the full Kn range, but it contains three empirical coefficients. The model proposed by Wu [15] weight superposition between slippage flow and Knudsen diffusion, however includes three empirical coefficients. Based on continuous flow and Knudsen diffusion, Rahmanian [41] proposed a bulk-gas transport model, which is suitable for nanopores with different cross-sections, and it includes three empirical coefficients. Notably, the determination of the weight coefficients requires a large number of accurate molecular simulation and experimental data, which seriously limits the application of the existing models in the development of shale gas in Guizhou Province. As a result, it is urgent to establish a universal bulk-gas transport model, which is free of empirical parameters.

2. Bulk-Gas Transport Mechanism

Knudsen number is defined as the ratio of the average free path of gas molecules to the scale of flowing medium, characterizing gas rarefaction [42]. Then, based on the Kn, Schaaf and Chambré divide the bulk transport mechanism of nanoporous gas into four basic types, namely, continuous flow, slippage flow, transition flow, and Knudsen diffusion [43]. Among them, it is still challenging to accurately describe the characteristics of transition flow.

$$Kn = \frac{\lambda}{d}, \tag{1}$$

where λ is the average free path of gas molecules, m, and d is the pore diameter of porous medium, m.

When $Kn < 0.001$, the gas transport mechanism is continuous flow, and the intermolecular collision dominates the transport process. At this point, the flow characteristics can be characterized by the nonslip Navier-Stokes equation. According to the Hagen-Poiseuille equation [15],

$$J_c = -\frac{r^2 p}{8\mu_g RT}\frac{dp}{dl}, \tag{2}$$

where J_c represents the flow capacity of continuum flow mechanism, mol/(m^2·s); r is the pore radius, m; p is the fluid flow pressure, Pa; μ_g is the gas viscosity, Pa·s; R is universal gas constant, J/(mol·K); T is the temperature, K; and l is the distance in the gas flow direction, m.

When the Kn is between 0.001 and 0.1, the gas nanopore transmission mechanism is slippage flow, the collision frequency between gas molecules and wall increases gradually, and the nonslippage condition of continuous flow breaks down. After decades of research at home and abroad, it is found that satisfactory results can be obtained by modifying the slip boundary conditions [44, 45].

$$J_s = -\frac{r^2 p}{8\mu_g RT}\left(1 + \frac{4Kn}{1 - bKn}\right)\frac{dp}{dl}, \tag{3}$$

where J_s is the transport capacity of gas slippage flow, mol/(m^2·s), and b is the gas slippage constant. When b is 0, it represents the first-order slippage condition, and when the value is -1, it represents the second-order slippage condition. Moreover, according to a large number of molecular simulation and experimental data, the fitting effect of the second-

order slippage condition is obviously better than that of the first-order, so the expression of nanopore phase transport of gas slippage flow can be simplified.

$$J_s = -\frac{r^2 p}{8\mu_g RT}\left(1 + \frac{4Kn}{1+Kn}\right)\frac{dp}{dl}. \tag{4}$$

When the Knudsen number is greater than 10, the transmission mechanism of gas nanopores is Knudsen diffusion, the collision frequency between gas molecules continues to decline, and the collision frequency between molecules and wall dominates the transmission process, which can be expressed by Knudsen equation [37, 39].

$$J_k = -\frac{d}{3}\sqrt{\frac{8}{\pi RTM}}\frac{dp}{dl}. \tag{5}$$

In view of the dominant collision between gas molecules and wall in this transmission mechanism, the influence of wall roughness on gas diffusion must be considered. The coarser the wall, the weaker the gas diffusion ability. The relationship can be characterized by the following formula [15, 43].

$$J_k = -\frac{d}{3}\delta^{D_f-2}\sqrt{\frac{8}{\pi RTM}}\frac{dp}{dl}, \tag{6}$$

where δ is the ratio of molecular diameter to local pore diameter, dimensionless, and D_f is the fractal dimension of pore wall, dimensionless. When the fractal dimension is 2, it represents a smooth wall and has no effect on the gas transmission capacity. When the fractal dimension is 3, it represents a rough wall.

3. Evaluation of Existing Gas Bulk Transport Models

3.1. Previous Contributions. Knudsen had proposed the bulk-gas transport model in the field of vacuum science, and it was widely used to describe the characteristics of transition flow and molecular free diffusion. However, using this model will overestimate the transport capacity of slippage flow, and Knudsen model contains two fitting parameters. In order to facilitate the comparison between the models in the following, the existing models are dimensionless [42]. The accuracy of the model at high Knudsen number is analyzed by the ratio of all Knudsen bulk phase model to Knudsen diffusion (J_a/J_k), and the accuracy of the model at low Knudsen number is analyzed by the ratio of all Knudsen bulk phase model to continuous flow (J_a/J_c). For Knudsen model,

$$\frac{J_{ak}}{J_k} = \frac{3\pi}{64Kn} + \frac{1 + 2.507(1/Kn)}{1 + 3.095(1/Kn)}, \tag{7}$$

$$\frac{J_{ak}}{J_c} = 1 + \frac{64Kn}{3\pi}\left(\frac{2.507}{3.095}\right). \tag{8}$$

In the above formula, J_{ak} characterize the gas transmission capacity proposed by Knudsen under the whole Kn range, mol/(m^2·s).

Adzumi studied the flow characteristics of mixed gas in capillary through a large number of experiments and proposed the use of weight factor to couple viscous flow and Knudsen diffusion to characterize full Knudsen flow for the first time [33–35]. It is proposed that the weight factor slowly increases from 0.7 to 1 with the decrease of pressure. When the pressure decreases to a very low level, the value is 1. At this time, molecular free diffusion is the main transmission form. Unfortunately, Adzumi did not give the specific expression of the weight factor.

$$J_{aa} = J_c + \varepsilon J_k. \tag{9}$$

In the above formula, J_{aa} characterize the gas transmission capacity proposed by Adzumi for the whole Knudsen number, mol/(m^2·s), and ε is the weight factor, dimensionless.

Beskok [32] modified the slippage flow by introducing the molecular rarefaction coefficient and extended the formula to the full Kn range. It can achieve good match with the molecular simulation data and experimental results, but it contains two empirical coefficients.

$$J_{ab} = -\frac{r^2 p}{8\mu RT}(1 + \alpha Kn)\left(1 + \frac{4Kn}{1 - bKn}\right)\frac{dp}{dl}, \tag{10}$$

$$\frac{J_{ab}}{J_k} = \frac{3\pi}{64Kn}(1 + \alpha Kn)\left(1 + \frac{4Kn}{1 - bKn}\right), \tag{11}$$

$$\frac{J_{ab}}{J_c} = (1 + \alpha Kn)\left(1 + \frac{4Kn}{1 - bKn}\right), \tag{12}$$

$$\alpha = \alpha_0 \frac{2}{\pi}\tan^{-1}\left(\alpha_1 Kn^{\beta}\right). \tag{13}$$

In the above formula, J_{ab} characterize the gas transmission capacity proposed by Beskok for the total Knudsen number, mol/(m^2·s); α is the gas rarefaction coefficient and increases with the increase of Kn. In this paper, α is 4 and β is 0.4. Figure 1 shows the variation curve of the gas sparsity coefficient with Knudsen number when α takes 1.19 and 1.358, respectively. Gas rarefaction coefficient increases slowly with the increase of Kn. When the Kn rises to a very high level, the coefficient remains basically unchanged. Moreover, for Beskok model, different fitting parameters will have a great impact on the calculation results, and the fitting parameters often need to be determined through a large number of experimental and molecular simulation data, which limits the practicability of the model.

Liu et al. [36] applied the concept of Adzumi weight factor, namely, formula (10), to simulate the gas slippage effect in porous media. Liu et al. believed that the thickness of slippage layer in different nanopores was different and used the

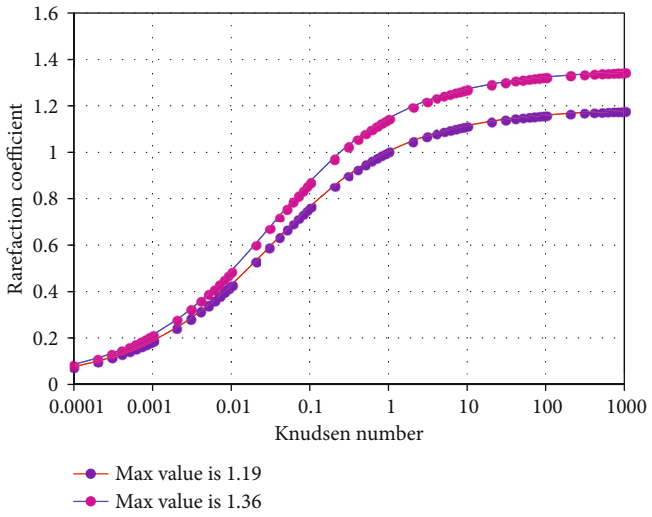

Figure 1: Gas rarefaction coefficient with different empirical factors.

weight factor to characterize the proportion of slippage layer in the flow channel.

$$\varepsilon = 4Kn - 4Kn^2, \tag{14}$$

$$\frac{J_{al}}{J_k} = \frac{3\pi}{128Kn} + 4Kn - 4Kn^2, \tag{15}$$

$$\frac{J_{al}}{J_c} = 1 + \left(4Kn - 4Kn^2\right)\frac{128Kn}{3\pi}. \tag{16}$$

In the above formula, J_{al} characterize the gas transmission capacity proposed by Liu et al. for the whole Knudsen number, mol/(m^2·s).

Javadpour [37] corrected the influence of slippage phenomenon on continuous flow transmission capacity through dimensionless coefficient proposed by Brown [46, 47] according to slippage flow and Knudsen diffusion and added them linearly to describe the transmission characteristics of gas in shale nanopores. Subsequently, Azom [38] and Darabi [48], respectively, considered the influence of real gas effect and wall roughness on the basis of the Javadpour's model. Since both Azom's and Darabi's model are based on Javadpour's model, only Javadpour's model and molecular simulation data need to be compared here.

$$\begin{aligned} J_{aj} &= FJ_c + J_k, \\ F &= 1 + \left(\frac{8\pi RT}{M}\right)^{0.5}\frac{\mu}{\mathrm{Pr}}\left(\frac{2}{\omega} - 1\right), \\ \frac{J_{aj}}{J_k} &= \left[1 + 8Kn\left(\frac{2}{\omega} - 1\right)\right]\frac{3\pi}{128Kn} + 1, \\ \frac{J_{aj}}{J_c} &= 1 + 8Kn\left(\frac{2}{\omega} - 1\right) + \frac{128Kn}{3\pi}. \end{aligned} \tag{17}$$

In the above formula, J_{aj} characterize the gas transmission capacity proposed by Javadpour, mol/(m^2·s); F is the tangential increment coefficient of gas molecular momentum, which represents the ratio of molecular viscous collision to mirror collision. This value varies from 0 to 1. Meanwhile, its determination depends on wall roughness, gas type, temperature, pressure, and many experimental results [49]. Dimensionless parameter F is always greater than 1, and when the bulk flow mechanism becomes continuous flow and slippage flow, the parameter maintains small. While flow mechanism becomes transition flow and Knudsen diffusion, the parameter increases with the increasing Kn.

Based on Adzumi's weight factor idea, Rahmanian [41] proposed the corresponding weight factor, coupled continuous flow and molecular diffusion, and established a bulk-gas transport model covering entire Kn range, but the model contains three fitting parameters.

$$\begin{aligned} J_{ar} &= (1 - \varepsilon)J_c + \varepsilon J_k, \\ \varepsilon &= C_A\left[1 - \exp\left(\frac{-Kn}{Knvisc}\right)\right]^S. \end{aligned} \tag{18}$$

In the above formula, J_{ar} characterizes the gas transmission capacity proposed by Rahmanian for the total Knudsen number, mol/(m^2·s). It is the critical Knudsen number, indicating that the slippage flow of the conveyor is transformed into molecular free diffusion, and both are fitting parameters. For nanoround holes, the corresponding fitting parameters C_A are K_{nvisc} 2.2, 0.3, and 5.

$$\begin{aligned} \frac{J_{ar}}{J_k} &= \left[1 - C_A\left(1 - \exp\left(\frac{-Kn}{Knvisc}\right)\right)^S\right]\frac{3\pi}{128Kn} \\ &\quad + C_A\left(1 - \exp\left(\frac{-Kn}{Knvisc}\right)\right)^S, \\ \frac{J_{ar}}{J_c} &= 1 - C_A\left(1 - \exp\left(\frac{-Kn}{Knvisc}\right)\right)^S \\ &\quad + C_A\left(1 - \exp\left(\frac{-Kn}{Knvisc}\right)\right)^S\frac{128Kn}{3\pi}. \end{aligned} \tag{19}$$

Based on slippage flow and Knudsen diffusion, Wu [15] proposed a model to weight superposition the above two mechanisms, in which ratio of intermolecular collision frequency and collision frequency between molecule and pore wall are set as the weight factor for slip flow mechanism and Knudsen diffusion, respectively. Formula for slip flow, proposed by Beskok, is utilized by Wu; therefore, the model proposed by Wu also contains three fitting parameters.

$$\varepsilon = \frac{Kn}{1 + Kn}, \tag{20}$$

$$\frac{J_{aw}}{J_k} = \frac{3\pi}{128\delta^{D_f-2}Kn}\left(1+\frac{4Kn}{1-bKn}\right)\frac{(1+\alpha Kn)}{1+Kn}+\frac{Kn}{1+Kn}, \tag{21}$$

$$\frac{J_{aw}}{J_c} = \left(1+\frac{4Kn}{1-bKn}\right)\frac{(1+\alpha Kn)}{1+Kn}+\frac{\delta^{D_f-2}Kn^2}{1+Kn}\frac{128}{3\pi}. \tag{22}$$

In the above formula, J_{aw} characterizes the gas transmission capacity proposed by Wu for the whole Knudsen number, mol/(m^2·s); α is the gas rarefaction coefficient.

3.2. Evaluation. In order to analyze the accuracy of each model, the calculated values of each model are compared with the results of molecular simulation [50]. The accuracy of the model at high Knudsen number is analyzed by the ratio of total Knudsen bulk phase model to Knudsen diffusion (J_a/J_k), and the accuracy of the model at low Knudsen number is analyzed by the ratio of total Knudsen bulk phase model to continuous flow (J_a/J_c). For the bulk-gas transmission of nanotubes under the full Kn range, the values of fitting parameters in the above model are shown in Table 1.

According to Figure 2, when Knudsen number is between 0.001 and 0.01, the ratio of existing bulk-gas transport model to continuous flow is close to 1, indicating that the bulk-gas transport capacity can be characterized by continuous flow equation when Knudsen number is low. As the Knudsen number continues to increase, the value continues to rise, showing the characteristics that slippage contributes to the transmission capacity. Among them, Javadpour's model rises the fastest and has the largest gap with the molecular simulation results, overestimating the bulk phase transmission capacity. Liu's model is consistent with the molecular simulation results when the Knudsen number is less than 0.1. When the Knudsen number is greater than 0.1, the calculated value of the model is higher than the molecular simulation results, indicating that Liu's model can characterize the characteristics of continuous flow and slippage flow but overestimate the transmission capacity of transition flow. The predicted value of Rahmanian's model underestimates the bulk-gas transmission capacity when the Knudsen number is less than 0.6 and overestimates the gas bulk phase transmission capacity when the Knudsen number is greater than 0.6. The trend of Knudsen's, Beskok's, and Wu's models is consistent with the molecular simulation results fairly well. Among them, Knudsen model slightly overestimates the bulk-gas transmission capacity. In Wu's model, when the Knudsen number is less than 0.3, the calculated value is slightly lower than the molecular simulation result, and when the Knudsen number is greater than 0.3, the calculated value is slightly higher than the molecular simulation result. Beskok's model performs best at low Knudsen number, and the error between Beskok's model and molecular simulation results is always the smallest.

According to Figure 3, due to the unreasonable expression of the weight factor of Liu's model, when Knudsen number is greater than 1, the weight factor is negative, so its predicted value cannot represent gas transmission capacity under high Knudsen number. Javadpour's and Raminian's model overestimates the bulk-gas transmission capacity by 2.2 times and 1.9 times at high Knudsen number. Knudsen's, Beskok's, and Wu's models fit well with the molecular simulation results. When Knudsen number is less than 10, the calculated value of Knudsen's model is slightly higher than the molecular simulation results, and the calculated value of Wu's model is lower than the molecular simulation results with a large error. When Knudsen number is greater than 10, the calculated results of the two models almost coincide and are slightly higher than the molecular simulation results. Beskok's model still performs best under high Knudsen number. When Kn is less than 1, the calculated value is slightly lower than that of molecular simulation. Comprehensive analysis of the comparison results between existing models and molecular simulation shows that Beskok's model shares the highest accuracy. However, the model contains three fitting parameters, which further highlights the necessity of establishing bulk-gas transmission model without fitting parameters. Comparing the establishment methods of the Beskok's model and Wu's model, it can be demonstrated that Beskok extends the slippage flow equation to the total Knudsen number by introducing gas sparsity effect, while Wu's model used the weight factor to

Table 1: The fitting parameters used in the calculation.

Fitting parameters	Numerical value	Fitting parameters	Numerical value
$\alpha_{0(Beskok)}$	1.358	C_A	2.2
α	4	K_{nvisc}	0.3
β	0.4	S	5
ω	0.8	$\alpha_{0(Wu)}$	1.19
δ	0.5	D_f	2.6

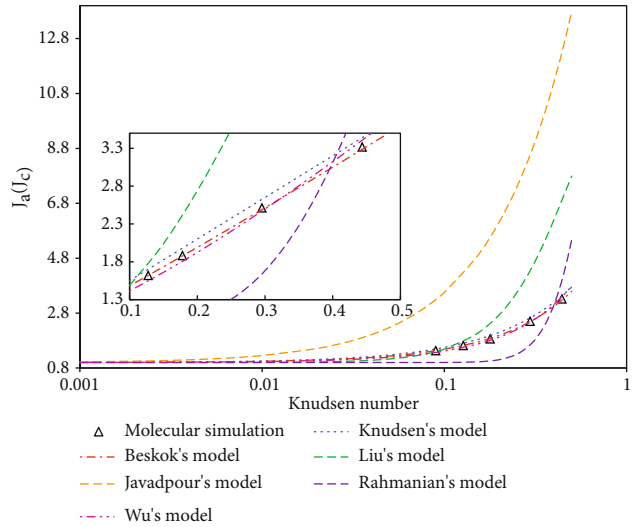

Figure 2: Comparison of existing models and molecular simulation results under low Kn.

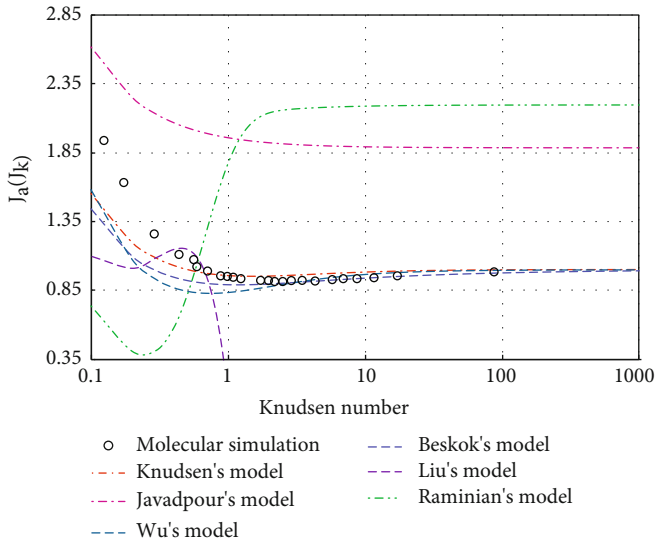

Figure 3: Comparison of existing models and molecular simulation results under high Kn.

couple the slippage flow and molecular diffusion. For Wu's model, the adopted slippage flow mechanism includes fitting parameters, eventually leading to establishment of the model relying on the fitting parameters. However, this kind of method is suitable for establishing the bulk-gas transmission model without fitting parameters.

4. Establishment of Bulk-Gas Transport Model

Through the comparison of the above models, it can be seen that there are four kinds of bulk-gas transmission models using the concept of weight factor. Among them, the weight factor of Liu's model is negative when the Knudsen number is greater than 1, which is obviously unreasonable. Javadpour's model and Raminian's model used weight factors to couple continuous flow and Knudsen diffusion. Because the gas slippage effect is not covered by their flow mechanism, these two models need to use weight factors with fitting parameters. Moreover, through the comparison, the errors of the two models are large, indicating that their weight factors are unreasonable. Wu's model couples slippage flow and Knudsen diffusion, and slippage flow contains the fitting parameters of Beskok's model. When Knudsen number is between 0.1 and 10, that is, transition flow, there is a large error between the calculated value of the model and molecular simulation, but its weight factor does not contain fitting parameters, and the model can accurately describe the characteristics of slippage flow. Therefore, formula (22) can be used to determine the weight factor of slippage flow in the proposed model in this article.

Knudsen's model is widely used in vacuum science and can accurately describe transition flow and molecular diffusion, which can also be obtained from the comparison in the previous section. Therefore, formula (8) can be used to determine the weight factor of Knudsen diffusion in the new model. Based on Wu's model and Knudsen's model, the weight factors of slippage flow and Knudsen diffusion

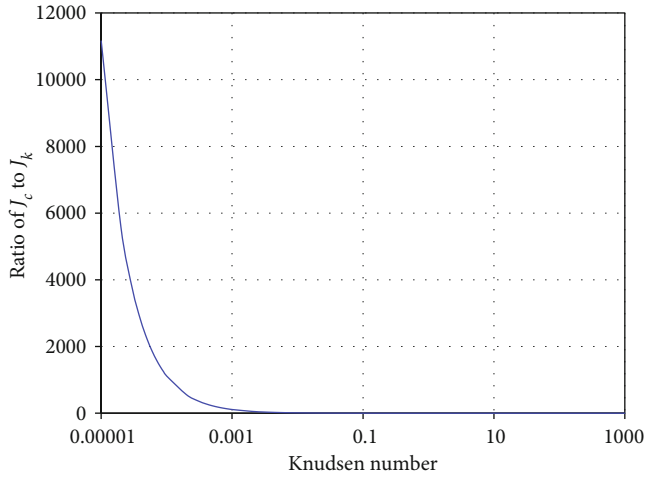

Figure 4: Ratio of continuous flow and Knudsen diffusion with different Kn.

are determined by referring to their expressions, respectively. Smooth nanopore surface is assumed; thus, the wall fractal dimension is 2.

$$J_{as} = \frac{1}{1+5Kn} J_s + \frac{Kn+2.507}{Kn+3.095} J_k, \tag{23}$$

$$\frac{J_{as}}{J_k} = \frac{3\pi}{128\delta^{D_f-2}Kn}\left(1+\frac{4Kn}{1+Kn}\right)\frac{1}{1+5Kn} + \frac{Kn+2.507}{Kn+3.095}, \tag{24}$$

$$\frac{J_{as}}{J_c} = \left(1+\frac{4Kn}{1+Kn}\right)\frac{1}{1+5Kn} + \frac{\delta^{D_f-2}(Kn+2.507)Kn}{Kn+3.095}\frac{128}{3\pi}. \tag{25}$$

In the above formula, J_{as} characterizes the gas transmission capacity proposed in this paper for the full Knudsen number, mol/(m^2·s).

$$\frac{J_c}{J_k} = \frac{3\pi}{128\delta^{D_f-2}Kn}. \tag{26}$$

The bulk-gas transport model without fitting parameters, proposed in this paper, can accurately describe the characteristics of each flow mechanism under entire Kn range. When the Knudsen number is very small, it can be seen from formula (3) that J_S will degenerate to J_C. It can be seen from Figure 4 that J_C is much greater than J_K; then, formula (24) will degenerate into a continuous flow equation at low Knudsen number. When Knudsen number is maximum, according to formula (24), J_{as} directly degenerates into Knudsen diffusion equation. When the flow mechanism is slippage flow and transition flow, it can be verified by comparing the calculated values of the model with the molecular simulation results and (J_a/J_C) and (J_a/J_K), respectively. The specific comparison results are shown in Figure 5. The analysis shows that the model can reach an excellent match with molecular simulation results, which shows that the proposed model can still be perfectly applicable in the slippage flow and transition flow. To sum up, the established nonfitting parameter bulk-gas transport model can accurately describe all flow mechanisms under the full Knudsen number, and its reliability has been verified. Because the model does not contain fitting parameters, it can be directly used to evaluate the gas transmission capacity under different reservoir conditions, demonstrating its simplicity and practicability.

5. Bulk-Gas Phase Transport Capacity during Shale Gas Development

In the development of oil and gas resources, the most important evaluation parameter of reservoir quality is permeability, which represents the gas transmission capacity. In conventional reservoirs, due to the absence of a large number of nanopores and high formation pressure, the general flow mechanism is continuous flow. In this case, the bulk phase transmission capacity is close to a constant. However, for unconventional reservoirs with massive nanopores, the gas transmission mechanism is generally slippage flow and transition flow, and its bulk phase transmission capacity depends on the formation pressure, temperature, and the corresponding pore scale, in which the temperature has little effect on the transmission capacity. In view of the continuous decrease of reservoir pressure in the development process, it is necessary to focus on the analysis of bulk-gas transmission capacity of different pore scales under different reservoir pressure conditions. In the following analysis, the gas is pure methane, and the reservoir temperature is set to 313 k.

It can be seen from Figure 6 that in the process of gas reservoir exploitation, the bulk-gas transmission capacity of different nanopores keeps an upward trend with the decrease of reservoir pressure, and the rising range is closely related to

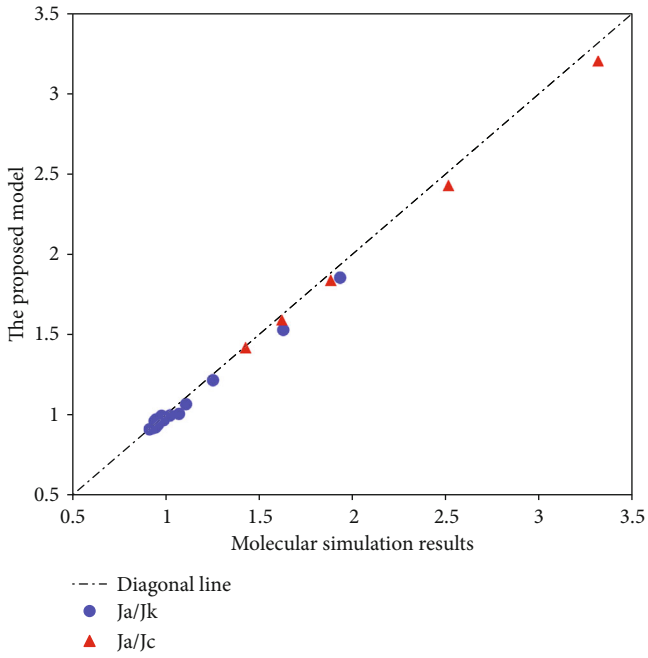

Figure 5: The comparison between proposed model and molecular simulation results.

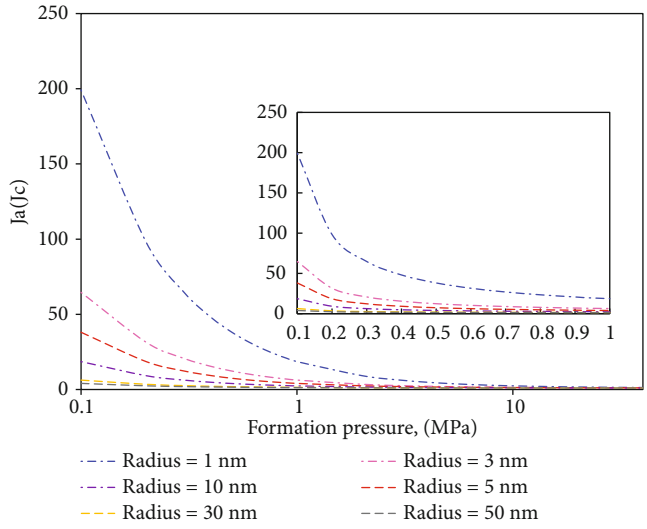

Figure 6: Gas transport capacity in different nanopores during the production process.

the pore scale. The smaller the pore radius is, the faster the bulk-gas transmission capacity is improved. When the local formation pressure is greater than 10 MPa, the bulk-gas transmission capacity can be characterized by continuous flow equation. When the pressure is between 1 and 10 MPa, the transmission capacity of nanopores with different scales increases slowly with the decrease of pressure. When the pressure is less than 1 MPa, the transmission capacity increases rapidly. For 1 nm pores, the transmission capacity is about 200 times that of continuous flow, and for 3 nm and 5 nm pores, it is about 60 times and 40 times. Once

the pore size exceeds 30 nm, its bulk phase transmission capacity is not sensitive to the change of reservoir pressure, and lifting range is no more than 6 times compared with continuous flow.

In view of the small variation range of pore transmission capacity greater than 30 nm with pressure, the transmission characteristics of pores above 30 nm will not be analyzed next. For the same pores, the contribution of slippage flow and Knudsen diffusion mechanism to the overall transmission capacity is different with the decrease of pressure. In this paper, the contribution factors of Knudsen diffusion and continuous flow to the overall transmission capacity of nanopores are defined as follows.

$$F_{ks} = \frac{1}{(1/1 + 5Kn)(Kn + 3.095/Kn + 2.507)(J_s/J_k) + 1},$$
$$F_{ss} = \frac{1}{1 + (1 + 5Kn)(Kn + 2.507/Kn + 3.095)J_k/J_s}. \quad (27)$$

The relationship between them and reservoir pressure is shown in Figure 7. When the reservoir pressure is between 10 and 40 MPa, the bulk-gas transmission greater than 3 nm is mainly contributed by slippage flow, but with the decrease of pressure, the contribution of slippage flow gradually decreases and the contribution of Knudsen diffusion gradually increases. When the reservoir pressure is less than 10 MPa, the contribution of slippage flow to pores larger than 3 nm decreases rapidly, and the contribution of Knudsen diffusion increases rapidly. When the pressure is 0.1 MPa, the bulk-gas transmission characteristics of such pores can be completely characterized by Knudsen diffusion. For pores with a radius of 1 nm, the contribution of each transport mechanism to the overall bulk phase transport capacity varies approximately linearly with the pressure, and when the reservoir pressure is 40 MPa, the contribution of Knudsen diffusion (0.31) is significantly higher than that of pores with a radius of 3 nm and above (0.12 and 0.08), indicating that the nanoscale bulk phase transport capacity and transport type are highly sensitive to the pore radius.

The transport characteristics of nanopores at full Knudsen number can be analyzed by the ratio of the established nonfitting parameter full Knudsen number bulk phase transport model to continuous flow and Knudsen diffusion. As shown in Figure 8, when the Knudsen number is extremely small, the value of (J_{as}/J_c) approaches 1, indicating that the continuous flow can be used to describe the flow characteristics of this stage. When Knudsen number is extremely large, value of (J_{as}/J_k) approaches 1. At this time, Knudsen diffusion can characterize the transmission characteristics. These are consistent with the existing understanding, which verifies the reliability of this model to a certain extent. According to the mechanism of slippage flow and transition flow, which are generally concerned, it can be seen from Figure 8 that the model in this paper also has high accuracy, so it can be used to analyze the flow characteristics in these two states. According to the analysis of Figure 8, (J_{as}/J_c) increases linearly with the increase of Knudsen number.

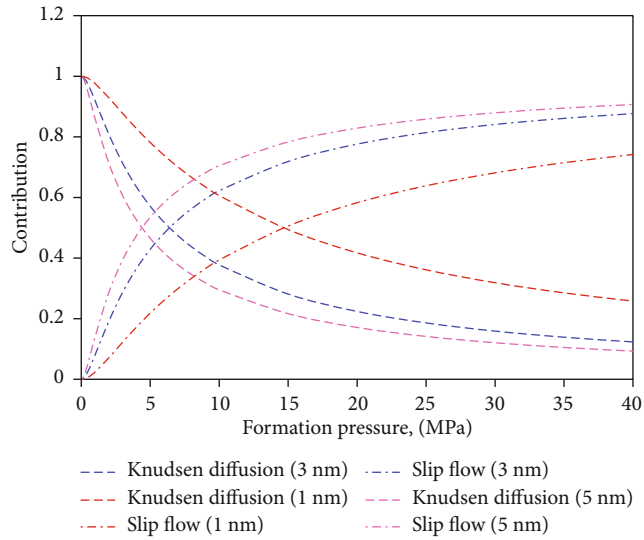

Figure 7: Contribution of different transport mechanisms during the production process.

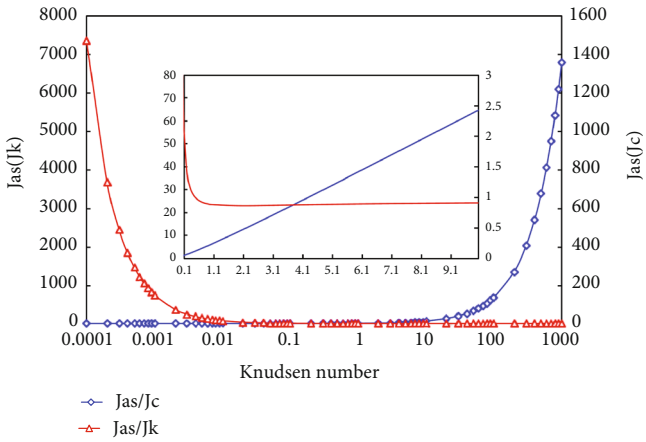

Figure 8: The bulk-gas transport capacity curve with different Knudsen number.

When the Knudsen number is less than 1, (J_{as}/J_k) decreases rapidly with the increase of Knudsen number. When the Knudsen number is greater than 1, the value no longer decreases and approaches 1. When the Knudsen number is greater than 10, the value is stable at 1. This shows that the change law of bulk phase transmission capacity changes in the transition flow stage, and the Knudsen number of 1 is the critical point of the change law.

6. Conclusions

(1) By comparing and analyzing previous models and molecular simulation data, it is found that Liu's model cannot characterize gas transmission capacity when Kn is greater than 1. Models, established by Javadpour and Raminian, overestimate the bulk-gas transmission capacity under high Kn. The Knudsen, Beskok, and Wu models can reach a favorable

match. When Kn is less than 10, the calculated results of Knudsen model are slightly higher than that of molecular simulation. Also, the calculated data of Wu's model underestimates the bulk-gas transmission capacity

(2) An analytical model of full Knudsen number gas bulk transport without fitting parameters is established for the first time. The model is suitable for accurately describing all flow mechanisms for the entire Kn range, and its reliability is verified by comparison with molecular simulation. Because the model does not contain fitting parameters, it can be directly used to evaluate the gas transmission capacity and field data processing under different reservoir conditions, which reflects its simplicity and strong practicability

(3) With the decrease of reservoir pressure, the transmission capacity of bulk-gas keeps an upward trend, and the rising range is closely related to the pore scale. The smaller the pore radius is, the faster the transmission capacity of bulk-gas is improved. In the process of gas reservoir exploitation, with the decrease of reservoir pressure, the contribution of slippage flow gradually decreases and the contribution of Knudsen diffusion gradually increases. By further analyzing the variation characteristics of bulk-gas transmission capacity in the transition flow, it is found that the Kn of 1 is the critical point of bulk-gas transmission capacity changing to Knudsen diffusion

Data Availability

Data are available on request.

Ethical Approval

On behalf of all the coauthors, the corresponding author states that there are no ethical statements contained in the manuscripts.

Conflicts of Interest

The authors declare that there is no conflict of interest regarding the publication of this paper.

Acknowledgments

The research acknowledges the financial support of Zunyi Normal University (BS-[2019]-20).

References

[1] C. Ruehl and J. Giljum, "BP energy outlook 2030," *Energy*, vol. 2030, no. 2, 2011.

[2] M. Yoshimune, T. Yamamoto, M. Nakaiwa, and K. Haraya, "Preparation of highly mesoporous carbon membranes via a sol–gel process using resorcinol and formaldehyde," *Carbon*, vol. 46, no. 7, pp. 1031–1036, 2008.

[3] Z. Sun, B. Huang, Y. Liu et al., "Gas-phase production equation for CBM reservoirs: interaction between hydraulic fracturing and coal orthotropic feature," *Journal of Petroleum Science and Engineering*, vol. 213, p. 110428, 2022.

[4] F. Xuehai, Q. Yong, and W. Chongtao, *Coalbed Methane Geology*, China University of mining and Technology Press, Xuzhou, 2003.

[5] C. Özgen Karacan, "Heterogeneous sorption and swelling in a confined and stressed coal during CO_2 injection," *Energy & Fuels An American Chemical Society Journal*, vol. 17, no. 6, pp. 1595–1608, 2003.

[6] H. Siriwardane, I. Haljasmaa, R. McLendon, G. Irdi, Y. Soong, and G. Bromhal, "Influence of carbon dioxide on coal permeability determined by pressure transient methods," *International Journal of Coal Geology*, vol. 77, no. 1–2, pp. 109–118, 2009.

[7] J. J. Howard, "Porosimetry measurement of shale fabric and its relationship to illite/smectite diagenesis," *Clays & Clay Minerals*, vol. 39, no. 4, pp. 355–361, 1991.

[8] T. J. Katsube, "Statistical analysis of pore-size distribution data of tight shales from the Scotian Shelf," *Current Research, Part E. Geological Survey of Canada, Paper*, vol. 92, 1992.

[9] R. M. Reed, R. G. Loucks, and D. M. Jarvie, "Nanopores in the Mississippian Barnett shale: distribution morphology, and possible genesis," *Gas Shales of North America*, vol. 39, 2007.

[10] F. P. Wang and R. M. Reed, "Pore networks and fluid flow in gas shales//Society of Petroleum Engineers," *SPE Paper*, no. - article 124253, 2009.

[11] P. H. Nelson, "Pore-throat sizes in sandstones, tight sandstones, and shales," *AAPG Bulletin*, vol. 93, no. 3, pp. 329–340, 2009.

[12] C. Cercignani and A. Daneri, "Flow of a rarefied gas between two parallel plates," *Journal of Applied Physics*, vol. 34, no. 12, pp. 3509–3513, 1963.

[13] Z. Sun, B. Huang, K. Wu et al., "Nanoconfined methane density over pressure and temperature: wettability effect," *Journal of Natural Gas Science and Engineering*, vol. 99, p. 104426, 2022.

[14] G. Sheng, Y. Su, and W. Wang, "A new fractal approach for describing induced-fracture porosity/permeability/compressibility in stimulated unconventional reservoirs," *Journal of Petroleum Science and Engineering*, vol. 179, pp. 855–866, 2019.

[15] W. Keliu, L. Xiangfang, and C. Zhangxin, "Real gas transport through nanopores of shale gas reservoirs," *China Science: Science and technology*, vol. 46, no. 1, pp. 68–78, 2016.

[16] J. C. Maxwell, "On stresses in rarefied gases arising from inequalities of temperature," *Proceedings of the Royal Society of London*, vol. 27, pp. 304–308, 1878.

[17] E. H. Kennard, *Kinetic Theory of Gases*, vol. 483, McGraw-hill, New York, 1938.

[18] W. A. Ebert and E. M. Sparrow, "Slip flow in rectangular and annular ducts," *Journal of Fluids Engineering*, vol. 87, no. 4, pp. 1018–1024, 1965.

[19] G. L. M. M. Spiga, "Slip flow in rectangular microtubes," *Nanoscale and Microscale Thermophysical Engineering*, vol. 2, no. 4, pp. 273–282, 1998.

[20] A. K. Sreekanth, "Slip flow through long circular tubes," *Rarefied gas dynamics*, vol. 1, pp. 667–680, 1969.

[21] E. S. Piekos and K. S. Breuer, "Numerical modeling of micromechanical devices using the direct simulation Monte Carlo

method," *Journal of Fluids Engineering*, vol. 118, no. 3, pp. 464–469, 1996.

[22] S. Chapman and T. G. Cowling, *The Mathematical Theory of Non-uniform Gases*, Cambrige University Press, Cambrige, 1952.

[23] G. E. Karniadakis and A. Bekok, *Microflows: Fundamentals and Simulation*, Springer, Berlin Heidelberg New York, 2002.

[24] R. G. Deissler, "An analysis of second-order slip flow and temperature-jump boundary conditions for rarefied gases," *International Journal of Heat & Mass Transfer*, vol. 7, no. 6, pp. 681–694, 1964.

[25] Y. Mitsuya, "Modified Reynolds equation for ultra-thin film gas lubrication using 1.5order slip-flow model and considering surface accommodation coefficient," *Transactions of the Japan Society of Mechanical Engineers C*, vol. 115, no. 2, pp. 289–294, 1993.

[26] J. Maurer, P. Tabeling, P. Joseph, and H. Willaime, "Second-order slip laws in microchannels for helium and nitrogen," *Physics of Fluids*, vol. 15, no. 9, pp. 2613–2621, 2003.

[27] S. Colin and P. L. R. Caen, "Validation of a second-order slip flow model in rectangular microchannels," *Heat Transfer Engineering*, vol. 25, no. 3, pp. 23–30, 2004.

[28] G. A. Bird, *Molecular Gas Dynamics and the Direct Simulation of Gas Flows*, Clarendon Press, Oxford, 1998.

[29] M. L. Hudson and T. J. Bartel, *DSMC Simulation of Thermal Transpiration and Accomodation Pumps (No. SAND-98-2015C; CONF-980765-)*, Sandia National Lab.(SNL-NM), Albuquerque, NM (United States), 1998.

[30] J. C. Harley, Y. Huang, H. H. Bau, and J. N. Zemel, "Gas flow in micro-channels," *Journal of Fluid Mechanics*, vol. 284, no. 284, pp. 257–274, 1995.

[31] S. Chen and G. D. Doolen, "Lattice Boltzmann method for fluid flows," *Fluid Mechanics*, vol. 30, no. 1, pp. 329–364, 1998.

[32] A. Beskok and G. E. Karniadakis, "Report: a model for flows in channels, pipes, and ducts at micro and nano scales," *Nanoscale and Microscale Thermophysical Engineering*, vol. 3, no. 1, pp. 43–77, 1999.

[33] H. Adzumi, "Studies on the flow of gaseous mixtures through capillaries. I The viscosity of binary gaseous mixtures," *Bulletin of the Chemical Society of Japan*, vol. 12, no. 5, pp. 199–226, 1937.

[34] H. Adzumi, "Studies on the flow of gaseous mixtures through capillaries. II. The molecular flow of gaseous mixtures," *Bulletin of the Chemical Society of Japan*, vol. 12, no. 6, pp. 285–291, 1937.

[35] H. Adzumi, "Studies on the flow of gaseous mixtures through capillaries. III. The flow of gaseous mixtures at medium pressures," *Bulletin of the Chemical Society of Japan*, vol. 12, no. 6, pp. 292–303, 1937.

[36] Q. Liu, P. Shen, and P. Yang, "Pore scale network modelling of gas slippage in tight porous media," *Fluid Flow and Transport in Porous Media: Mathematical and Numerical Treatment*, vol. 295, pp. 367–375, 2002.

[37] F. Javadpour, "Nanopores and apparent permeability of gas flow in mudrocks (shales and siltstone)," *Journal of Canadian Petroleum Technology*, vol. 48, no. 8, pp. 16–21, 2009.

[38] P. N. Azom and F. Javadpour, "Dual-continuum modeling of shale and tight gas reservoirs," in *SPE annual technical conference and exhibition*, San Antonio, Texas, USA, 2012.

[39] H. Singh, F. Javadpour, A. Ettehadtavakkol, and H. Darabi, "Nonempirical apparent permeability of shale," *SPE Reservoir Evaluation & Engineering*, vol. 17, no. 3, pp. 414–424, 2014.

[40] R. F. Aguilera, J. F. Ramirez, and C. E. Ortega, "A variable shape distribution (VSD) model for characterization of pore throat apertures and drill cuttings in tight and shale reservoirs," in *SPE Asia Pacific Oil and Gas Conference and Exhibition*, Perth, Australia, 2012.

[41] M. R. R. Shahri, R. Aguilera, and A. Kantzas, "A new unified diffusion-viscous flow model based on pore level studies of tight gas formations," *SPE Journal*, vol. 18, no. 1, pp. 38–49, 2012.

[42] M. Knudsen, "Die Gesetze der Molekularströmung und der inneren Reibungsströmung der Gase durch Röhren," *Annalen der Physik*, vol. 333, no. 1, pp. 75–130, 1909.

[43] S. A. Schaaf and P. L. Chambré, *Flow of Rarefied Gases*, Princeton University Press, 1961.

[44] Z. Sun, B. Huang, Y. Li, H. Lin, S. Shi, and W. Yu, "Nanoconfined methane flow behavior through realistic organic shale matrix under displacement pressure: a molecular simulation investigation," *Journal of Petroleum Exploration and Production Technology*, vol. 12, no. 4, pp. 1193–1201, 2022.

[45] Z. Sun, S. Wang, H. Xiong, K. Wu, and J. Shi, "Optimal nanocone geometry for water flow," *AICHE Journal*, vol. 68, no. 3, p. 17543, 2022.

[46] B. D. Eldridge and L. F. Brown, "The effect of cross sectional pore shape on Knudsen diffusion in porous materials," *AICHE Journal*, vol. 22, no. 5, pp. 942–944, 1976.

[47] S. L. Matson and J. A. Quinn, "Knudsen diffusion through noncircular pores: textbook errors," *AICHE Journal*, vol. 23, no. 5, pp. 768–770, 1977.

[48] A. Ettehad, F. Javadpour, and K. Sepehrnoori, "Gas flow in ultra-tight shale strata," *Journal of Fluid Mechanics*, vol. 710, no. 12, pp. 641–658, 2012.

[49] H. W. de Regt, "The Scientific Letters and Papers of James Clerk Maxwell," *Journal of China Coal Society*, vol. II, pp. 1862–1873, 1996.

[50] S. K. Loyalka and S. A. Hamoodi, "Poiseuille flow of a rarefied gas in a cylindrical tube: solution of linearized Boltzmann equation," *Physics of Fluids A Fluid Dynamics*, vol. 2, no. 11, pp. 2061–2065, 1990.